Atmospheric Environment 254 (2021) 118390

Contents lists available at ScienceDirect

Atmospheric Environment

journal homepage: http://www.elsevier.com/locate/atmosenv

Black carbon emissions from flaring in Russia in the period 2012–2017

Kristin Böttcher [a,*], Ville-Veikko Paunu [a], Kaarle Kupiainen [b], Mikhail Zhizhin [c], Alexey Matveev [d], Mikko Savolahti [a], Zbigniew Klimont [e], Sampsa Väätäinen [f], Heikki Lamberg [f], Niko Karvosenoja [a]

[a] Finnish Environment Institute (SYKE), Latokartanonkaari 11, FI-00790, Helsinki, Finland
[b] Ministry of the Environment (YM), Aleksanterinkatu 7, FI-00023, Government, Finland
[c] Colorado School of Mines, 1500 Illinois Street, Golden, CO, 80401, United States
[d] National University of Oil and Gas "Gubkin University", Leninskiy Prospekt, 65, 119296, Moscow, Russia
[e] International Institute for Applied Systems Analysis (IIASA), Schlossplatz 1, A-2361, Laxenburg, Austria
[f] Fine Particle and Aerosol Technology Laboratory, Department Environmental and Biological Sciences, University of Eastern Finland, Yliopistonranta 1, FI-70211, Kuopio, Finland

HIGHLIGHTS

- New estimate for black carbon emissions from flaring in Russia.
- Enhanced temporal profiles of flared gas volume from VIIRS.
- Oil and gas field-type specific emission factors developed.
- Average BC emissions from 2012 to 2017 are estimated at 68.3 Gg/year.

GRAPHICAL ABSTRACT

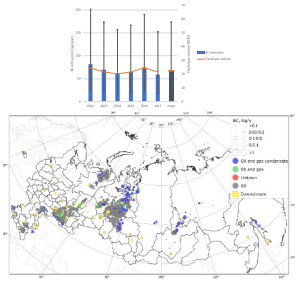

ARTICLE INFO

Keywords:
Black carbon
Emissions
Gas flaring
Russia
Visible infrared imaging radiometer suite (VIIRS)

ABSTRACT

Gas flaring in the oil and gas industry has been identified as an important source of anthropogenic black carbon (BC) affecting the climate, particularly in the Arctic. Our study provides spatially-explicit estimates of BC emissions from flaring in Russia utilising state-of-the-art methodology for determining the emission factors. We utilised satellite time series of the flared gas volume from Visible Infrared Imaging Radiometer Suite (VIIRS) for the period 2012 to 2017, supplemented with information on the gas and oil field type. BC emissions at flaring locations were calculated based on field type-specific emission factors, taking into account different gas compositions in each field type. We estimate that the average annual BC emissions from flaring in Russia were 68.3 Gg/year, with the largest proportion stemming from oil fields (82%). We observed a decrease in the yearly emissions during the period 2012 to 2017 with regional differences in the trend. Our results highlight the importance of detailed information on gas composition and the stage of oil and gas separation of the flared gas to reduce uncertainties in the BC emission estimates.

* Corresponding author.
E-mail addresses: Kristin.Bottcher@syke.fi (K. Böttcher), Ville-Veikko.Paunu@syke.fi (V.-V. Paunu), Kaarle.Kupiainen@ym.fi (K. Kupiainen), mzhizhin@mines.edu (M. Zhizhin), matveevhwre@gmail.com (A. Matveev), Mikko.Savolahti@syke.fi (M. Savolahti), klimont@iiasa.ac.at (Z. Klimont), sampsa.vaatainen@uef.fi (S. Väätäinen), heikki.lamberg@uef.fi (H. Lamberg), Niko.Karvosenoja@syke.fi (N. Karvosenoja).

https://doi.org/10.1016/j.atmosenv.2021.118390
Received 15 September 2020; Received in revised form 22 March 2021; Accepted 30 March 2021
Available online 2 April 2021

1. Introduction

Gas flaring is the burning of associated petroleum gas (APG) in the oil extraction industry. Although APG is a form of natural gas and can be utilised correspondingly after being processed, it is often flared instead (IEA, 2019). According to satellite estimates, globally about 145 billion cubic meters (BCM) of gas was flared in 2018 (The World Bank, 2019) corresponding to 350 million tons of CO_2 equivalent emissions per year. During flaring, air pollutants, such as black carbon (BC), SO_2, NO_X and CO, are released to the atmosphere, influence the Earth's radiative balance and can have a warming or cooling impact on climate (AMAP, 2015; Shindell et al., 2012). In the Arctic, BC is considered as a key pollutant inducing positive climate forcing (Bond et al., 2013). BC affects the Arctic climate via several mechanisms: (i) the atmospheric burdens contribute to direct heating of air, (ii) the deposition and concentrations in snow and ice reduce the surface albedo and accelerate the melting processes (Hadley and Kirchstetter, 2012) and iii) BC as a component of aerosols interacts with clouds (Bond et al., 2013; Kühn et al., 2020), affecting their formation, distribution, size and radiative properties (Boucher et al., 2013). Several studies have suggested that BC from flaring can be a significant factor contributing to Arctic warming (AMAP, 2015; Cho et al., 2019; Sand et al., 2016). BC emissions from flaring are estimated to account for about one third of emissions north of 60°N and two thirds north of 66°N; the emissions occur mostly in oil fields in the Russian territory (Stohl et al., 2013, 2015). BC measurements on a ship campaign in the Arctic Ocean, complimented with simulated concentrations, showed that major flaring sites have a significant impact on local BC concentrations in the Arctic (Popovicheva et al., 2017).

According to The World Bank (2019), the amount of gas flared in 2018 in Russia was 21.3 BCM. Russian oil resources are mainly located in West Siberia and the Urals-Volga region. The largest oil producing region, accounting for 45% of the production in 2016, is the Khanty-Mansiysk area located in West Siberia. In 2016, about 12% of oil was produced in East Siberia and Russia's Far East (U.S. Energy Information Administration, 2017). Estimates of Russian BC emissions from anthropogenic sources indicate flaring of APG as the largest source sector, with the other main sectors being transport, agricultural waste burning and residential combustion (Evans et al., 2017; Huang et al., 2015; IIASA, 2020; Klimont et al., 2017). The contribution of flaring to the Russian total BC emissions has been estimated at 36% (Huang et al., 2015) or 46% (Conrad and Johnson, 2017). The emission estimates are burdened with uncertainties due to lack of, for example, emission measurement data from Russian flaring sites as well as missing facility-level activity data (see e.g. Huang et al. (2015)).

Satellite remote sensing provides information that can be used to derive spatial distribution and trends of gas flaring worldwide, including the Arctic. The satellite detection of flares is based on their radiative emissions. Currently, no instrument exists that was specifically designed for the detection of flares. In most cases, night-time images from medium resolution instruments, such as the Visible Infrared Imaging Radiometer Suite (VIIRS) (Elvidge et al., 2016; Zhang et al., 2015), the Along Track Scanning Radiometer (ATSR/AATSR), the Sentinel-3 Sea and Land Surface Temperature Radiometer (SLSTR) (Casadio et al., 2012; Caseiro et al., 2018, 2020) and the Moderate Resolution Imaging Spectroradiometer (MODIS) (Anejionu et al., 2015; Faruolo et al., 2018) have been utilised for the mapping of gas flares. All these instruments measure in the wavelength range of peak radiant emissions of flares at about 1.6 μm (Elvidge et al., 2016; Fisher and Wooster, 2018). Due to the moderate spatial resolution of the satellite observations, flares cover, in fact, only a small fraction of the pixel's footprint (~500 m^2 to ~1 km^2).

Globally consistent estimates of annual flared gas volumes have been made from VIIRS since 2012 (Elvidge et al., 2016). For this, the satellite estimates have been calibrated against country-reported data on gas flaring (Elvidge et al., 2016). These VIIRS-based estimates are utilised for the reporting of the amount of gas flaring by the World Bank's Global Gas Flaring Reduction Partnership (The World Bank, 2020). VIIRS Nightfire products showed better suitability for the detection of flares than the MODIS thermal anomaly products in Khanty-Mansiysk, Russia (Sharma et al., 2017). Furthermore, the derived flare source area from the VIIRS Nightfire algorithm correlated well with interpretations of Google Earth imagery (Sharma et al., 2017). Good accuracy of VIIRS Nightfire flared gas volume at offshore sites compared to reported values was found by Brandt (2020).

While remote sensing has been utilised to detect flaring locations and to provide estimates on the source temperature, the radiant heat and gas volume of the observed flares (Caseiro et al., 2018; Elvidge et al., 2016), emission factors are usually applied to convert the activity data (such as the flared gas volume) to emissions (Klimont et al., 2017). The BC emissions depend on the composition of the APG and the combustion process (Bond et al., 2004), which is affected, for example, by wind speed and the operating conditions of flares (exit velocity, flare size and tip design) (Evans et al., 2017; Huang et al., 2015; McEwen and Johnson, 2012). Detailed information about the emission factors is scarce, and can be based on laboratory (McEwen and Johnson, 2012) or field measurements (Conrad and Johnson, 2017). This data is very limited, since it is only based on a small number of individual flares (Johnson et al., 2013) or from a flaring region (Gvakharia et al., 2017). Recently, satellite methods are also advancing towards the estimation of fire combustion efficiency, e.g. the potential for detection of the combustion phase of fires from VIIRS was shown by Wang et al. (2020).

Our objective was to calculate black carbon emissions from flaring in Russia based on satellite observations from VIIRS for the period 2012–2017. In this study, spatially-explicit information on the type of field was used for the first time to improve black carbon emission estimates from flaring. In addition, gas composition data of the APG in Russia was collected from the literature for different field types and applied together with the revised emission factor function from Conrad and Johnson (2017). We characterise spatial and interannual variability and BC emissions of flaring in Russian oil and gas fields. Furthermore, we derive uncertainty ranges for the estimated black carbon emissions and compare our results to the reported values in the literature.

2. Material and methods

An overview of datasets used and analysis conducted for estimating BC emissions in Russia is presented in Fig. 1. Details of the methods are described in the following sections.

2.1. Satellite observations of flared gas volume

We utilised satellite-observed flared gas volume from VIIRS Nightfire data that are available at the Colorado School of Mines (https://payneinstitute.mines.edu/eog/) for the period 2012–2017. The data are open source and readily available. The radiant heat (RH) of flares was derived from estimated flare temperature and source area using the Stefan–Boltzmann law. The subpixel flare source area was derived based on the Planck Curve (Elvidge et al., 2016). The yearly sum of RH for all gas flares in the country obtained with VIIRS Nightfire was used to calibrate a linear regression versus the annually reported flaring volumes from Cedigaz (Elvidge et al., 2016). This calibration against country level flared gas volume was then re-distributed back between individual flares in the oil and gas fields according to the flare annual RH estimate. For 2012, the VIIRS Nightfire data covering the period April–December were extrapolated to obtain annual estimates of RH.

2.2. Verification and enhancement of satellite observations

To obtain consistent time series of flaring sites in Russia, the locations were verified and tracked through the observation period 2012–2017 (Fig. 1, Step 1). For this purpose, every detected flare in

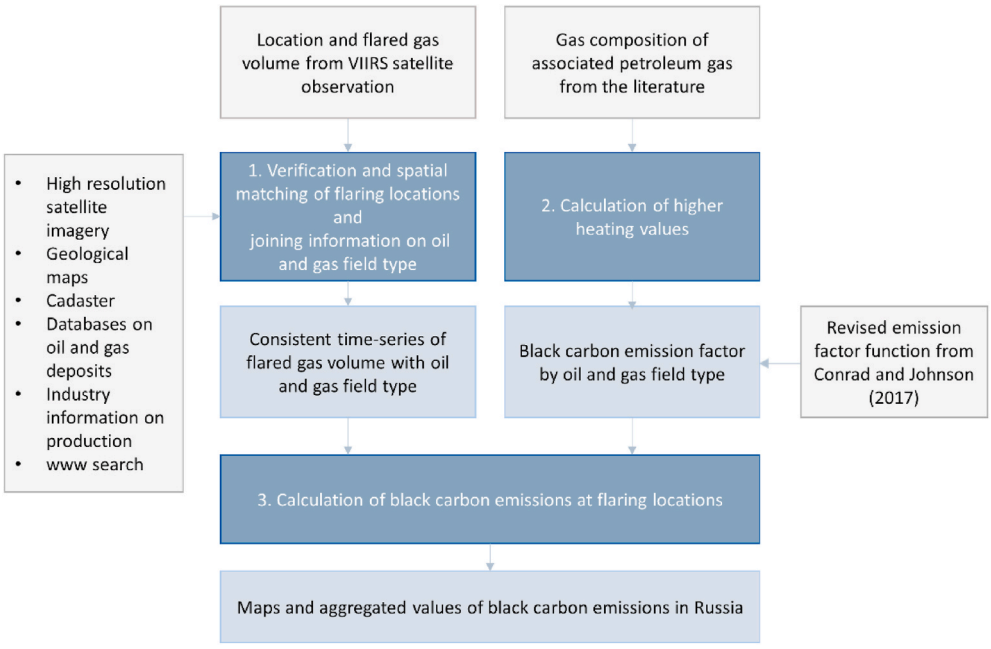

Fig. 1. Flowchart of datasets and analysis steps for the estimation of black carbon emissions.

Russia was then verified via high resolution daytime satellite images available in Google Earth. Several areas in Russia, however, did not have any available high-resolution coverage in Google Earth. In this case, images available at terraserver.com (https://terraserver.com/)[1] for the period 2017–2019 were utilised. When no images were found, the detected heat sources within oil and gas fields boundaries (obtained from Research and Analytical Center "Mineral" Map of mineral deposits in Russia (Online GeoMaps of the Russian Federation (Open version), 2002) were assumed to be a gas flare if they had a high percentage of detection within the last year (10% or more) or if they were related to oil and gas industry objects identified in the Public Cadastral Map of Rosreestr (Federal Service for State Registration, Cadaster and Cartography of Russia) (2011) or Wikimapia (Wikimapia).

In the following, information on the oil and gas field type was joined with the verified satellite-detected flaring locations. Several additional information sources were utilised for this purpose and the details of the procedure are given below. Data on the oil and gas deposits of Russia (Online GeoMaps of the Russian Federation (Open version), 2002) include geolocation and the field name. To identify deposit type, public information from the Rosgeolfond database (Rosgeolfond (Russian Federal Geological Fund)) was used. Rosgeolfond states the type of every deposit as an abbreviation (e. g., «НГКМ» is an abbreviation for 'Oil and Gas Condensate Deposit'). Around half of the deposits are labelled as just 'Oil Deposits', which were categorised as Oil deposits in this study; the same procedure was applied to 'Gas' and 'Gas Condensate' fields, although there are only a few of these deposits in Russia. Merely half of the deposits left were categorised as mixed deposits with the main produced component unknown.

To overcome this issue, several approaches were used.

1) Geography. Yamalo-Nenets Autonomous Okrug concentrates 85% of gas production of Russia and 20% of the world.[2] Therefore, most of the mixed fields in this region may be categorised as 'gas deposits', although oil may be produced alongside gas and gas condensate, like in case of the gigantic Urengoy field. However, oil production rates in this case will be far lower than gas production. Still, there are examples of relatively large mixed fields (such as Pyakyakha oil and gas condensate field), where oil and gas production ratios are close to each other; for this type of field, no primary component is stated. On rare occasions, the source of flaring in a mixed field may be recognised according to the type of engineering facility (available in Rosreestr (Federal Service for State Registration Cadastre and Cartography of Russia) (2011)) or (Wikimapia)).
2) Major oil and gas companies usually present the levels of production per major fields. This information may be available online (e. g., the Novatek company presents production and reserves info on its official website: http://www.novatek.ru/en/business/producing) or reported in annual reports (e.g., Rosneft not only presents the production rates in their annual reports (Rosneft), but in the last years, the volumes of flared APG by the main subsidiaries are presented).
3) Other cartographic sources that may contain additional supportive information, such as the Hydrocarbon Province Maps of Russia (Blackbourn Consulting), Harvard Oil & Gas Maps (Harvard University) and GIS Atlas "Subsoil of Russia" (A. P. Karpinsky Russian Geological Research Institute (VSEGEI)) were used.
4) If there was no information found via the mentioned methods, any available information on the field production rates or deposits was looked up on the internet. Sometimes the information may be presented in mass media (oil and gas specialised sources or regional media), in scientific research papers (primarily on geology) of the fields, or in annual reports on the economic activity of the region.
5) If there was still no metadata found about the flare, its type is marked as 'Unknown'.

The above methodology is based primarily on open-source data. To our knowledge, there is no single open-source table with such information on oil and gas field classification available in Russia.

The observed gas flares were divided into upstream and downstream (Elvidge et al., 2018). Upstream flares are located at the oil and gas fields, i.e. close to the production sites. Downstream flares are related to processing plants and sites. We merged gas and gas condensate fields with the class oil and gas condensate field into one category (Table 1).

[1] Terraserver stopped providing high-resolution images in 2020.
[2] https://expert.ru/russian_reporter/2014/35/sokrovischa-vechnoj-merzlotyi/.

2.3. Black carbon emission factors for gas flaring

For the calculation of emission factors, we applied the relationship between the heating value of the APG and black carbon emissions (Conrad and Johnson, 2017; McEwen and Johnson, 2012; Conrad and Johnson, pers. communication),

$$EF_{BC} = 0.0112(\ln(HHV - 37.6))^{4.612} + 0.194, \forall\, HHV > 38.6$$
$$EF_{BC} = 0.194, \forall\, \leq 38.6 \quad (1)$$

where EF_{BC} is the gas flaring BC emission factor (g/m^3) and HHV the higher volumetric heating value (MJ/m^3). The power law model in equation (1) provides a better fit to the available field and laboratory observations than the linear equation presented in Conrad and Johnson (2017). Furthermore, it avoids negative predictions at low heating values (Conrad and Johnson, pers. communication).

The higher volumetric heating value was calculated based on the composition of APG in Russia that was collected from the literature (Fig. 1, Step 2, Supplementary materials, Table S1). For upstream flares, the gas composition of the flared gas is typically different from the composition of the produced gas. It differs by field type and varies over time, depending of the depletion of the reservoir (PFC Energy, 2007). Typically, the methane content of the APG of an oil field is lower and the volumetric heating value is higher (65.49 MJ/m^3, Number of observations (N) = 6) when compared to oil and gas or oil and gas condensate fields (49.97 MJ/m^3, N = 7) (Supplementary materials, Table S1). Additionally, the heating value varies for the stages of oil and gas separation, i.e. the separation of the hydrocarbon mixture into two phases (oil and gas). In the field, the stage separation is usually carried out in several steps using a series of separators that operate at subsequently reduced pressures. Stage separation aims at maximised production and enhanced properties of the oil or condensate. The number of stages may vary, but three steps were found effective in most cases (Adewum, 2020). Traditionally, gas from stage 1 has been easiest to use and therefore has been less often flared than gas at stages 2 and 3 (Energas, 2016). However, the amount of gas that is utilised from stage 2 and 3 has increased with the raising of fines for gas flaring that came into force in 2012 in Russia (Energas, 2018). Due to the lack of information on the proportion of flaring at different stages, we applied the average of the volumetric heating value of the different stages of separation per field type. BC emission factors (Table 2) were then calculated from the average higher heating value per field type using equation (1).

2.4. Calculation of black carbon emissions and uncertainty

The amount of BC emissions from gas flaring in Russia was estimated for the average period 2012–2017 and for each year separately. For that, the emission factor for the respective field type (Table 2) was multiplied with the satellite-observed flared gas volume (section 2.1) at each flaring location (Fig. 1, Step 3). For gas and gas condensate fields, we assigned the same emission factor as for oil and gas condensate fields. For downstream flares and flares of unknown type, the average higher heating value of 59.83 MJ/m^3 of all available APG compositions (Supplementary materials, Table S1) was applied. Thus, according to equation (1), an EF_{BC} of 2.27 g/m^3 was used for downstream flares. Estimated BC emissions were aggregated by administrative region and for the whole country.

We calculated the uncertainty in BC emissions in Russia by year and for the average period 2012–2017 following Evans et al. (2017). Uncertainty sources in remote sensing observations of the flared gas volume are signal contaminations by clouds and natural light and scaling errors due to the larger satellite footprint compared to the flare size. The temporal sampling of VIIRS is adequate for steady and continuous flares, but intermittent and rarely active flares are under-sampled and the detection of small flares is challenging as they are usually detected in a single band (Elvidge et al., 2016). Thus, the modelling of temperature and source area based on Planck curve fitting is not feasible for small flares.

Here, an uncertainty range of ±9.5% was applied for the flared gas volume from VIIRS satellite observations (Elvidge et al., 2016; Evans et al., 2017). This range is based on the calibration of RH against country-reported values (see 2.1). We calculated the uncertainty in the annual flared gas volume for each field type of upstream and for downstream flares separately. To estimate the uncertainty in the BC emission factor for upstream flares, we utilised the range of emission factors for the specific field types (Table 2). For downstream flares, we applied the range of the calculated emission factors from all available gas composition data in Russia (0.19–12.17 g/m^3, Supplementary materials, Table S1). Thus, we estimated the lower bound of the uncertainty range in BC emissions by applying the lower bound of the flared gas volume and the minimum of the emission factor by field type. The upper bound of the uncertainty range was derived accordingly by using the upper bound of the flared gas volume and the highest emission factor for the respective field type.

Table 1
Number of flares per field type from VIIRS satellite observations.

Upstream				Downstream
Oil	Oil and Gas	Oil and gas condensate	Unknown	
831	146	1405	32	165

3. Results

From 2012 to 2017, the annual average BC emissions from Russian flaring were 68.3 Gg/year, with 64.1 and 4.2 Gg/year from upstream and downstream flares, respectively. There was a slight decreasing trend in the annual emissions (Fig. 2), but variation was high, as the highest emissions were for 2012, 81.4 Gg/year, and the lowest for 2017, 58.9 Gg/year. The uncertainties in BC emissions ranged from 21.13 to 148.79 Gg/year for upstream and from 0.33 to 24.93 Gg/year for downstream flares for the average period 2012 to 2017 (Table 3). Most emissions came from flares in oil fields (Fig. 3), representing 82% of the emissions on average, although comprising only 32% of the number of flares (Table 1) and 41% of flared gas volume. Oil and gas condensate represented 10% of the emissions and 45% of flared gas volume, oil and gas 2%, and 6%, and downstream flares 6%, and 8%, respectively. From 2012 to 2017, the emissions decreased by a higher percentage than the flared gas volume. This is due to flared gas volumes decreasing in oil fields. The flaring volumes from oil and gas condensate fields were highest in 2016 and 2017 and showed an increasing trend. As the emission factor was significantly lower in oil and gas condensate fields than in oil fields, the oil fields drove the changes in the emissions.

Fig. 4 and Fig. 5 show the spatial distribution of the mean BC emissions per flare, categorised by field type. Annual regional emissions are presented in Fig. 6. Khanty-Mansiysk had the highest emissions, representing about 40% of the total emissions on average. Orenburg, Yamal-Nenets and Tomsk were the regions with the next highest emissions, with shares of 10%, 8% and 7% of total emissions, respectively.

In several regions there was a decreasing trend, although in 2016 in many of these the emissions increased temporarily. Examples of these regions were Khanty-Mansiysk, Tomsk and Komi. In some regions, e.g. Yamal-Nenets and Orenburg, there were high emissions in 2012, strong decrease in the next one or two years and an increasing trend after that. Other regions, such as Irkutsk and Nenets showed a clearer increasing trend. Flares closest to the Arctic were in Yamal-Nenets and Nenets, and they had the 3rd and 6th highest average emissions from all regions. In Nenets, we observed a small spatial shift of flaring locations and emissions from south to north from 2012 to 2017 (not shown).

Table 2
Higher heating values (HHV) that were utilised for the calculation of black carbon emission factors (EF_{BC}) from Russian flaring locations. The composition of associated petroleum gas at the stages of oil and gas separation was obtained from Filippov (2013) and Chernov (2016) (see Supplementary materials, Table S1). Ranges in the HHV and the EF_{BC} due to different stages of oil and gas separation are given in brackets.

Field type	Oil		Oil and gas		Oil and gas condensate	
HHV (MJ/m^3)	86.81	[60.10–131.02]	49.12	[42.01–54.42]	47.32	[39.22–59.79]
EF_{BC} (g/m^3)	6.13	[2.30–12.17]	0.88	[0.26–1.54]	0.69	[0.19–2.26]

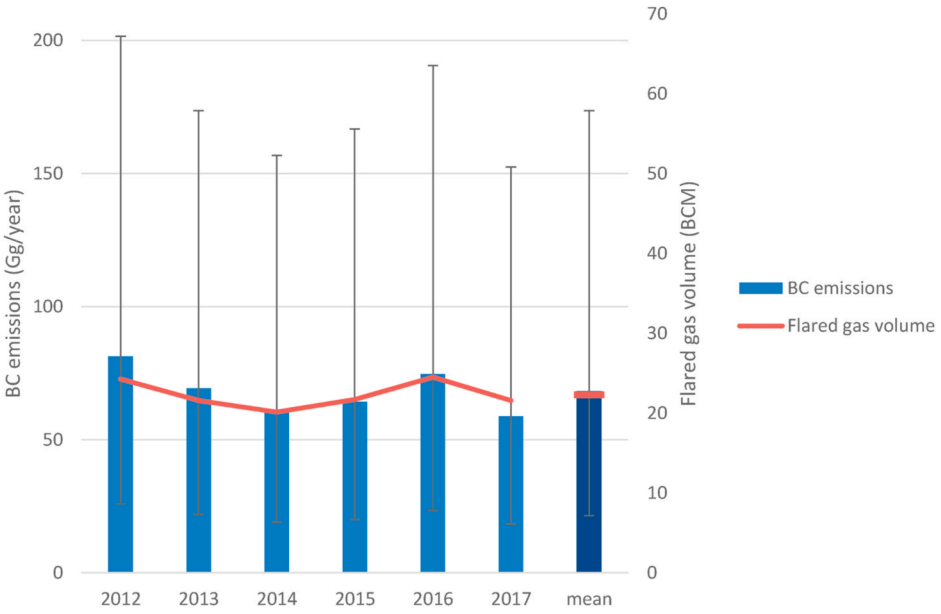

Fig. 2. Annual black carbon emissions with uncertainty ranges from Russian flaring and volume of the gas flared.

Table 3
Uncertainty in black carbon (BC) emissions for the average period 2012–2017 stemming from the uncertainty in the flared gas volume and emission factors. Overall uncertainty includes both sources of uncertainty.

	Field type	Average BC emissions (Gg/year)	Uncertainty from flared gas volume (Gg/year)	Uncertainty from emission factor (Gg/year)	Overall uncertainty (Gg/year)
Upstream	**Oil**	56.01	50.69–61.33	21.06–111.26	19.06–121.83
	Oil and gas	1.20	1.08–1.31	0.36–2.08	0.32–2.27
	Oil and gas condensate	6.84	6.19–7.49	1.93–22.43	1.75–24.56
	Unknown type	0.02	0.02–0.02	0.00–0.11	0.00–0.12
Downstream		4.24	3.84–4.64	0.36–22.77	0.33–24.93
All flares		68.31	61.82–74.79	23.71–158.64	21.47–173.61

4. Discussion

Flaring has been estimated to be a major source of BC emissions and the largest source in the high Arctic (Klimont et al., 2017; Stohl et al., 2013). Despite its significance, there are still large uncertainties associated with the emissions. The Arctic climate is more sensitive to local emissions than those from lower latitudes, and, therefore, these sources need to be better understood. New studies, such as this paper, help to assess the magnitude of the emissions (Fig. 2). In addition to emission estimates, the satellite observations provide information on the spatial distribution of flares (Figs. 4 and 5) that can be utilised to create a spatial proxy for global flaring emissions modelling, such as is done with the GAINS model (IIASA, 2020).

Reported BC emissions in Russia vary widely (Table 4), highlighting large uncertainties associated with the estimates. In global emission estimates from the GAINS model, ECLIPSEv6b (IIASA, 2020) and v5a (Klimont et al., 2017), the BC emissions for 2015 were similar to our calculation, both for the average and especially our estimate for 2015 (61.7 Gg/year, Fig. 2). However, ECLIPSEv5a had 65% higher flared gas volume and 42% lower emission factor than our study, so similar results were more of a coincidence. Huang et al. (2015) calculated BC emissions for 2010 as 81 Gg/year. The higher BC emissions in their study were mainly caused by higher flared gas volumes in 2010 compared to the period 2012 to 2017. Their emission factor was based solely on oil fields. However, it was lower than in our study due to differences in both the weighting of oil and gas separation stages and the emission factor equation from McEwen and Johnson (2012). Based on an update of the emission factor equation with field measurements, Conrad and Johnson (2017) suggested a higher BC emission factor for Russian oil fields (Table 4). The lowest BC emission estimate was from Caseiro et al. (2020) with 10 Gg/year for 2017.

Previous assessments, except Caseiro et al. (2020), were based on only one average BC emission factor for Russia. Our analysis of gas composition data from different field types (Table 2) suggested that lower emission factors for oil and gas and gas condensate fields, compared to oil fields, would be more appropriate. However, the

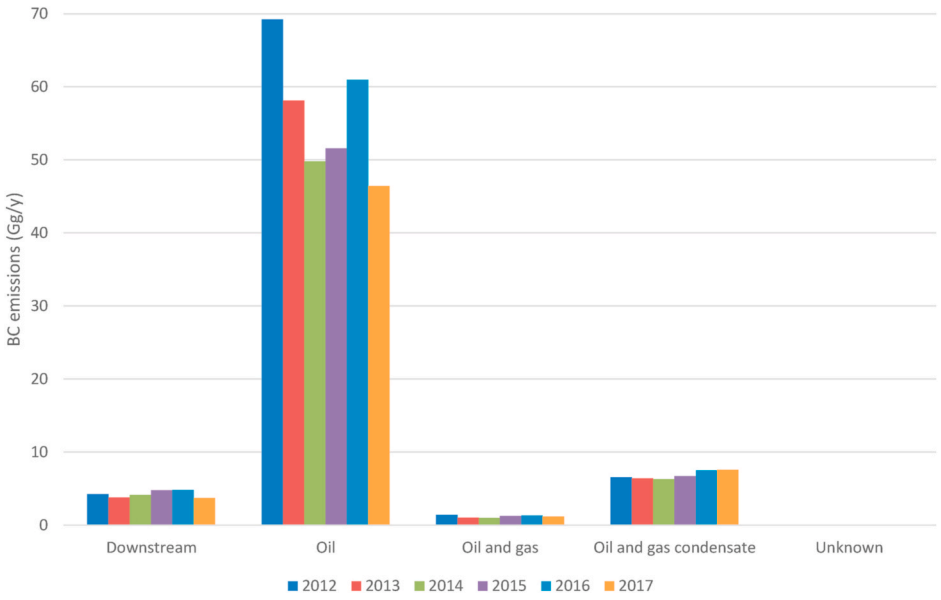

Fig. 3. Flaring black carbon emissions in Russia per field type.

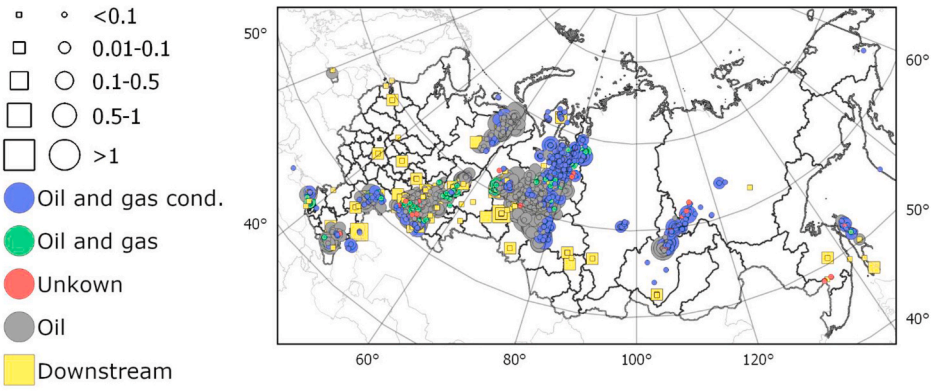

Fig. 4. Mean black carbon emissions (Gg/year) from individual flares in Russia for the period 2012–2017. The circles represent upstream flares and squares downstream flares. A high-resolution image of this map is provided in Supplementary Materials, Figure S1.

collected field data on APG composition from Russia (Supplementary Materials Table S1) is still limited and more field samples would be needed to ascertain this finding.

Fig. 7 shows the comparison of the spatial distribution of the BC emissions from our study to Huang et al. (2015) and ECLIPSEv6b (IIASA, 2020). In both cases, our results were aggregated to the same resolution as the comparison data. The spatial distribution of flaring emissions in ECLIPSEv6b is based on the same VIIRS nightfire data as our results, thus the locations of the emissions were similar. Spatial differences in the magnitude of the emissions are due to the spatially varying emission factor in our study compared to ECLIPSEv6b. In our data, the highest emissions were located in the oil production regions (see also Figs. 4 and 5). In ECLIPSEv6b there are some high emission grid cells further north, which are dominated by oil and gas condensate fields. Compared to Huang et al. (2015), our data showed additional emission sources in some regions, such as in Perm and Samara. According to our study, oil production areas in Khanty-Mansiysk stand out with higher emissions, whereas in Huang et al. (2015) the areas with high emissions were more evenly distributed, due to a single emission factor for all field types, and the emissions are spread to larger areas around hot spots.

In our estimates the total flared gas volume in Russia decreased from 2012 to 2014, increased then until 2016, and decreased again in 2017 (Fig. 2). The emissions followed the same path but decreased more than the flared gas volume. According to the U.S. Energy Information Administration (EIA) (2020), oil production in Russia increased from 10.6 million barrels per day in 2012 to 11.2 in 2017. This indicates that Russia was able to decrease flaring while increasing oil production. Regarding flared gas volumes, regional data published by the Federal State Statistics Service of Russia (Rosstat,[3,4]) (Fig. 8) show lower values than our data (or other scientific assessments listed in Table 4). Only in the Siberian and Far Eastern federal districts before 2015 Rosstat reported higher flared volumes. The overall trend is similar to our data, hence, supporting our finding that the flared gas volume decreased during the period 2012–2017. The increase from 2014 to 2016, seen in our data, is not present in the Rosstat data.

The observed decline of emissions might partly be explained by an increase in the utilisation rate[5] (Evans et al., 2017) and easier market

[3] Rosstat, Production of main types of products in physical terms from 2010 to 2016 [In Russian], available online: https://fedstat.ru/indicator/40557 (accessed on 18.12.2020).

[4] Rosstat, Production of main types of products in physical terms since 2017 [In Russian], available online: https://fedstat.ru/indicator/58636 (accessed on 18.12.2020).

[5] Information on the APG utilisation rate beyond year 2014 was not presented in Evans et al., (2017).

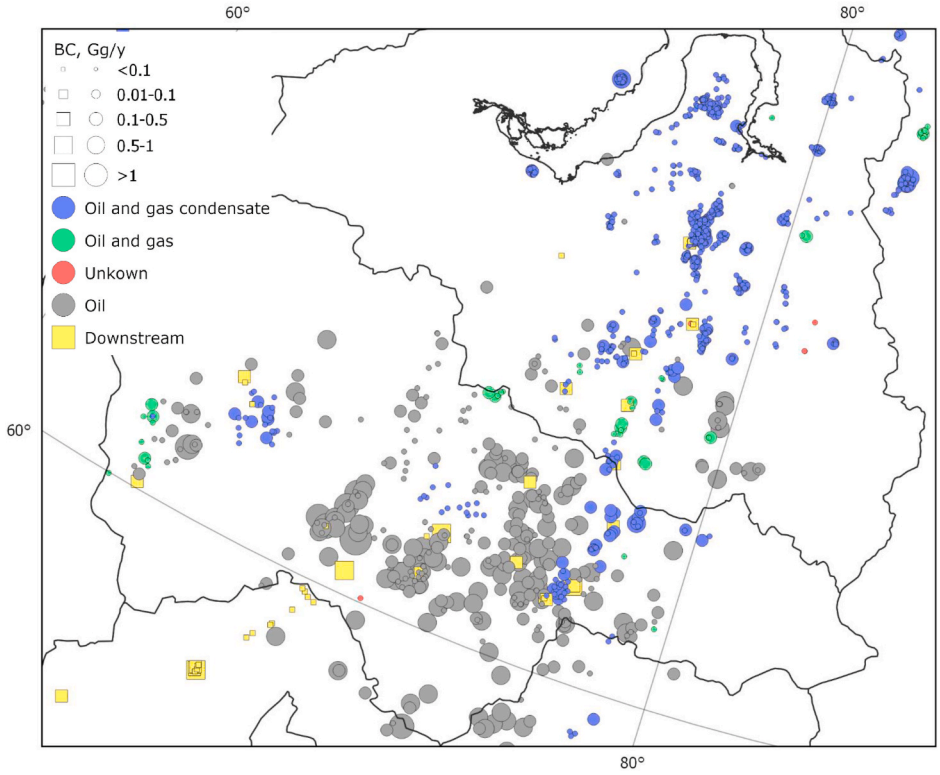

Fig. 5. Zoomed in on Khanty-Mansiysk and Yamal-Nenets regions with mean black carbon emissions from individual flares.

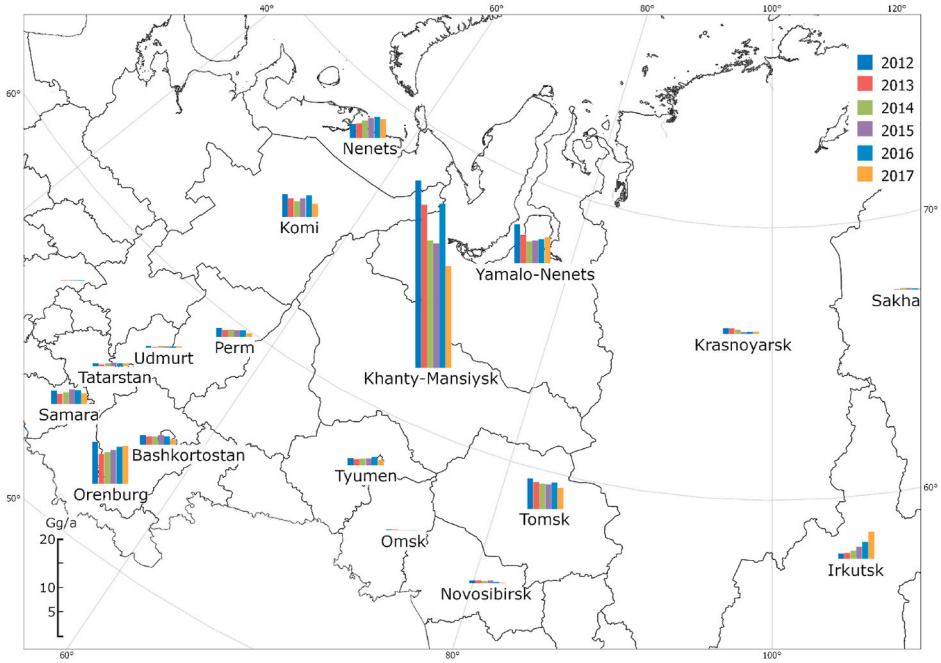

Fig. 6. Map of regional yearly flaring black carbon emissions from selected Russian regions.

access for APGs (Evans and Roshchanka, 2014). The Russian Federation requires oil companies to achieve a utilisation rate of 95% for the APG (Energas, 2018) and the metering of all flared gas since 2012 with accompanying legislation (Government of Russian Federation, 2009, 2012). High fines apply for flaring of APG exceeding this target. There are several measures available that can be used to reduce the BC emissions from flaring, as described by Saunier et al. (2019). It is unclear how widely the techniques have been implemented in Russia, but our results indicate that further reductions should be targeted to oil production sites.

Although we utilised improved spatially-explicit data for the calculation of the BC emissions, the estimates are highly uncertain (Table 3). The largest source of uncertainty in our results (~90%) stems from the uncertainty in the emission factors that is related to the heating value of the APG and other factors, such as flare technologies and local conditions, including atmospheric conditions. Heavier gas with a higher

Table 4
Black carbon (BC) emission estimates from flaring in Russia from different studies.

Assessment	Year	BC emission (Gg/year)	Uncertainty (%)	Flared gas volume (BCM)	Average emission factor (g/m^3)
Our study	2012–2017	68.3	31–254	22.3	3.06
ECLIPSEv6b (IIASA, 2020)	2015	65.3	–	23.8	2.78[a)]
ECLIPSEv5a (Klimont et al., 2017)	2015	61.9	–	36.8[b)]	1.76
Huang et al. (2015)	2010	81.0	66–240	35.6	2.27
Evans et al. (2017)	2014	32.2	31–168		1.67
Caseiro et al. (2020)	2017	10.0	50–150	18.0[c)]	0.56
Conrad and Johnson et al. (2017)	2010	123.0[d)]	–	35.6	3.46

[a)] The heating value of APG for Russia was revised to 65.2 MJ/m^3 using data from Huang et al. (2015) and a relationship from Conrad and Johnson (2017) used to derive a new emission factor. Data on flaring volumes as estimated by Höglund-Isaksson et al. (2020).

[b)] It was a projection based on the Energy Technology Perspectives (IEA, 2012) projections of oil and gas production in Russia (the value was similar to 2010).

[c)] The estimate is based on Sentinel-SLSTR data. Emission factor range was bound to ranges used in Klimont et al. (2017).

[d)] The calculation was based on the Higher Heating Value of associated petroleum gas in Russia by Huang et al. (2015), but revising the emission factor equation with additional field measurements.

heating value produces larger BC emissions (Conrad and Johnson, 2017, 2019; McEwen and Johnson, 2012). To our knowledge, there are no field measurements of BC emissions from Russian flare sites available in the literature. The applied emission factor function (equation (1)) is therefore based on field and laboratory measurements from North and South America. Some information on the composition of APG in Russia was nevertheless available. However, most of the data come from the Khanty-Mansiysk Autonomous Okrug in Western Siberia. Thus, other production areas are underrepresented (Supplementary Materials Table S1). Spatial and temporal variations in APG composition were found to be high in small areas in other regions (Conrad and Johnson, 2017; Johnson et al., 2013).

In addition, differences in heating values for the subsequent stages of oil and gas separation are even more important. Gas composition data for the different stages from Russia suggest that flaring at stage 3 could multiply BC emissions per BCM by a factor of 5 in oil fields and by a factor of 12 in oil and gas condensate fields (Table 2). The proportions of flaring at the different stages are unknown (CarbonLimits, pers. communication). Huang et al. (2015) and Evans et al. (2017) assumed that the majority of flaring occurs at stage 1. A larger proportion of flaring at the first stage in upstream flares would reduce the BC emissions in our results significantly. For example, when accounting for 70% of flaring at stage 1 and an equal distribution for the later stages, total BC emission estimates would reduce by 23.16 Gg/year or 34% for the period 2012 to 2017. Furthermore, the highest HHV in measurements by Conrad and Johnson was 71.29 MJ/m^3. For the Russian oil fields, the highest HHV for stage 3 APG was 131.02 MJ/m^3. Thus, equation (1) was extrapolated in our analysis. As this extrapolating is taken to far higher HHV than in the experimental data used in Conrad and Johnson (2017), the uncertainty increases with high HHV.

The spatial distribution of emission factors could potentially be further improved based on remote sensing observations. For example, Caseiro et al. (2020) used the satellite-derived flaring temperature as an indicator of the completeness of combustion and as the basis to scale emission factors between flares. Progress on the retrieval of combustion phase of fires from satellite observations was made by Wang et al. (2020) by using the visible energy fraction (the ratio of visible light power to fire radiative power). In their study, the visible energy fraction was correlated with a measure of combustion efficiency from the global fire emission database (https://www.globalfiredata.org/). The retrieval of combustion efficiency of different flares is also one important development direction for the VIIRS Nightfire algorithm.

In our analysis, the uncertainty in the flared gas volume from satellite observation was a minor contributor to the overall uncertainty of BC emissions. Applying the global uncertainty range of the flared gas volume of ± 9.5% (Elvidge et al., 2016) resulted in an uncertainty range of ± 6.5 Gg/year in Russia (Table 3). The flared gas volume in 2017 from Sentinel SLSTR by Caseiro et al. (2020) was lower (3.6 BCM or 16.5%, see Table 4) than retrievals from VIIRS Nightfire in 2017. The differences in the country-aggregated value could mainly be due to a stronger persistency criterion for the detection of flares and less observation opportunities caused by the smaller swath and an earlier overpass time of Sentinel-SLSTR compared to VIIRS (Caseiro et al., 2020). In a comparison of VIIRS Nightfire flared gas volume at offshore sites with government reported data from 9 countries, the accuracy was higher (±5%) for aggregated estimates (Brandt, 2020) than the applied uncertainty range in this study. Further work is needed for the accuracy assessment of land-based flare estimates (Brandt, 2020). Currently, the calibration of satellite-observed flared gas volumes against field data from flaring locations is ongoing. Measurements of the flared gas volumes and concurrently observed VIIRS signals from large test flare facilities, such as at the John Zinc testing facility in Oklahoma, could reduce calibration errors and allow better characterisation of the uncertainties of the satellite observations (Zhizhin et al., 2019) in future work.

5. Conclusions

We estimated BC emissions from flaring in Russia for 2012–2017. Our analysis was based on new field-type specific emission factors that were applied to VIIRS observations of the flared gas volume at individual flaring locations. On average for the period 2012 to 2017 the emissions were 68.3 Gg/year, from which 64.1 Gg/year were from upstream (with uncertainty range from 21.13 to 148.79 Gg/year) and 4.2 Gg/year from downstream flares (uncertainty range from 0.33 to 24.93 Gg/year). The major part, 82%, of the emissions came from flares in oil fields. The oil fields comprised only 41% of the total flared gas volume, indicating the importance of field type distinction for flaring emission assessments. Mean annual emission estimates were mostly in line with previous studies. However, our average emission factor was higher than in most other studies, mainly due to applying a new emission factor function and higher heating values for the flared gas in oil fields, making the similarity to some studies coincidental. Emissions showed high interannual variability, with 2012 having the highest BC emission of 81.4 Gg/year and 2017 the lowest with 58.9 Gg/year. Regionally, Khanty-Mansiysk had the highest emissions, representing on average 40% of the total flaring emissions in Russia. While the total emissions had a slight decreasing trend, regional emissions showed more variation. In addition to the new emission estimates, our results show the spatial distribution of the emissions. Taking field type into account was especially important for the spatial distribution, as major emissions were located at oil production fields.

Our results reinforce the importance of flaring in oil and gas extraction as a BC source close to the Arctic. While our results indicate a decreasing trend in the Russian flaring emissions, there remains large potential for emission reduction in the sector. According to our analysis, especially flaring in oil fields and at higher processing stages should be targeted with reduction measures. While our results are based on the

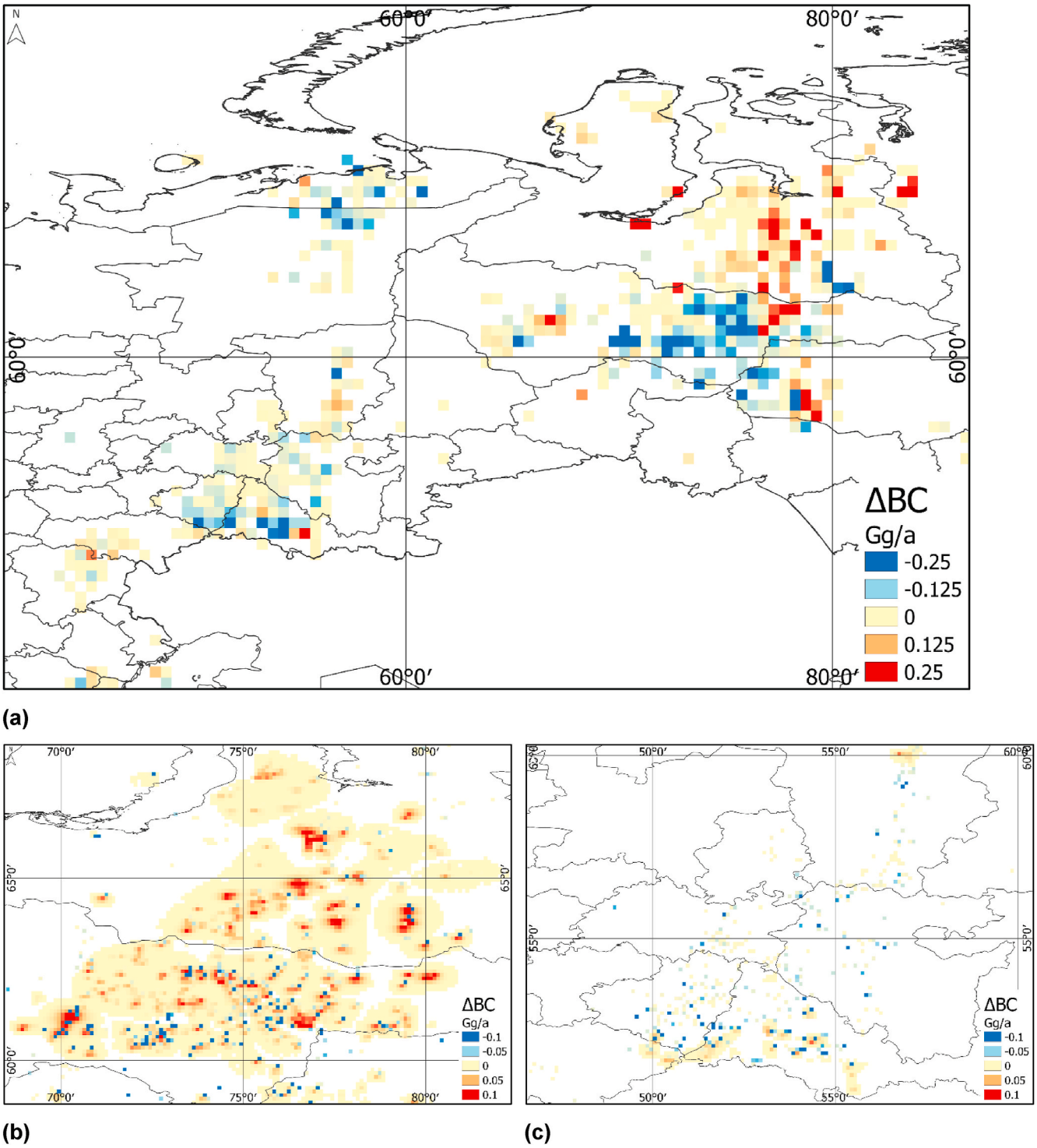

Fig. 7. Difference in the spatial distribution of black carbon emissions from (a) ECLIPSEv6b and our study in central Russia, and Huang et al. (2015) and our study in (b) Khanty-Mansiysk and Yamalo-Nenets regions and (c) Samara, Perm, Bashkortostan and Orenburg regions. The spatial grid resolution is 0.5° in (a) and 0.1° in (b) and (c). Blue indicates that our study had higher emission and red that the comparison study had higher emission in the cell.

latest knowledge from satellite observations and emission factors, significant uncertainties remain associated with the flaring emissions. In order to reduce the uncertainties, emission factors that better represent the actual emissions are needed. This would require measurements of BC emissions at individual flares, detailed gas composition profiles, documentation of different stages of oil and gas separation from fields in Russia and the consideration of the effect of climate conditions on BC emissions.

Data availability

Black carbon emissions estimates from flaring in Russia were made available at the Mendeley data repository at the following link: DOI:10.17632/wwkrw3p9xt.1. The published data set contains the coordinates of the flaring locations, the flared gas volume from VIIRS and the estimated black carbon emission for 2012–2017.

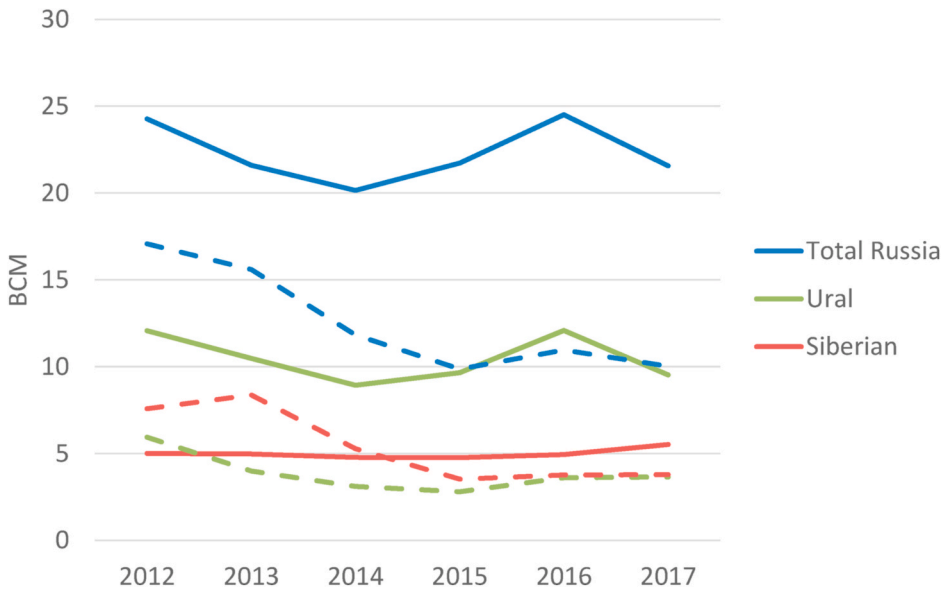

Fig. 8. Flared gas volumes for whole Russia, and for Ural and Siberian, the federal districts with the highest flared gas volumes. Solid lines are based on our data and dashed lines from the Federal State Statistic Service of Russia (Rosstat[3,4]).

CRediT authorship contribution statement

Kristin Böttcher: Conceptualization, Methodology, Formal analysis, Visualization, Writing – original draft, Writing – review & editing. **Ville-Veikko Paunu:** Conceptualization, Methodology, Formal analysis, Visualization, Writing – original draft, Writing – review & editing. **Kaarle Kupiainen:** Conceptualization, Supervision, Writing – review & editing. **Mikhail Zhizhin:** Methodology, Writing – review & editing. **Alexey Matveev:** Methodology, Writing – original draft, Writing – review & editing. **Mikko Savolahti:** Writing – review & editing. **Zbigniew Klimont:** Writing – review & editing. **Sampsa Väätäinen:** Writing – review & editing. **Heikki Lamberg:** Writing – review & editing. **Niko Karvosenoja:** Project administration, Funding acquisition, Writing – review & editing.

Declaration of competing interest

The authors declare that they have no known competing financial interests or personal relationships that could have appeared to influence the work reported in this paper.

Acknowledgements

This work was supported by the European Union (EU Action – Black Carbon in the Arctic/EUA-BCA; PI/2017/392–687); Academy of Finland (NABCEA; 296644), Business Finland (BC Footprint; 1462/31/2019) and by the Ministry for Foreign Affairs of Finland (IBA -project Black Carbon in the Eurasian Arctic and Significance Compared to Dust Sources; No. PC0TQ4BT-25).

We are grateful to Brad Conrad and Matthew Johnson (Carleton University, Ottawa, Canada) for providing us with updated information on black carbon emission factors from flaring and advice for the calculation of heating values of associated petroleum gas. We thank CarbonLimits (Norway) for information on gas composition and stages of oil and gas separation and three anonymous reviewers for their helpful comments and suggestions.

Appendix A. Supplementary data

Supplementary data to this article can be found online at https://doi.org/10.1016/j.atmosenv.2021.118390.

References

A. P. Karpinsky Russian Geological Research Institute (VSEGEI). GIS Atlas "Subsoil of Russia" [In Russian]. Available online. http://atlaspacket.vsegei.ru/. accessed on 03.10.2019.

Adewum, M., 2020. Phase Relations in Reservoir Engineering, Design and Optimization of Separators. Penn State College of Earth and Mineral Sciences. John A. Dutton e-Education Institute available online. https://www.e-education.psu.edu/png520/m20_p3.html. (Accessed 29 June 2020).

AMAP, 2015. AMAP Assessment 2015: Black Carbon and Ozone as Arctic Climate Forcers. Arctic Monitoring and Assessment Programme (AMAP), Oslo, Norway, p. 116 available online. https://www.amap.no/documents/doc/amap-assessment-2015-black-carbon-and-ozone-as-arctic-climate-forcers/1299. (Accessed 10 June 2020).

Anejionu, O.C.D., Blackburn, G.A., Whyatt, J.D., 2015. Detecting gas flares and estimating flaring volumes at individual flow stations using MODIS data. Rem. Sens. Environ. 158, 81–94.

Blackbourn Consulting, Hydrocarbon Province Maps. Available online: https://www.blackbourn.co.uk/databases/hydrocarbon-province-maps/, accessed on 03.10.2019.

Bond, T.C., Streets, D.G., Yarber, K.F., Nelson, S.M., Woo, J.-H., Klimont, Z., 2004. A technology-based global inventory of black and organic carbon emissions from combustion. J. Geophys. Res.: Atmospheres 109.

Bond, T.C., Doherty, S.J., Fahey, D.W., Forster, P.M., Berntsen, T., DeAngelo, B.J., Flanner, M.G., Ghan, S., Kärcher, B., Koch, D., Kinne, S., Kondo, Y., Quinn, P.K., Sarofim, M.C., Schultz, M.G., Schulz, M., Venkataraman, C., Zhang, H., Zhang, S., Bellouin, N., Guttikunda, S.K., Hopke, P.K., Jacobson, M.Z., Kaiser, J.W., Klimont, Z., Lohmann, U., Schwarz, J.P., Shindell, D., Storelvmo, T., Warren, S.G., Zender, C.S., 2013. Bounding the role of black carbon in the climate system: a scientific assessment. J. Geophys. Res.: Atmospheres 118, 5380–5552.

Boucher, O., Randall, D., Artaxo, P., Bretherton, C., Feingold, G., Forster, P., Kerminen, V.-M., Kondo, Y., Liao, H., Lohmann, U., Rasch, P., Satheesh, S.K., Sherwood, S., Stevens, B., Zhang, X.Y., 2013. Clouds and aerosols. In: Stocker, T.F., Qin, D., Plattner, G.-K., Tignor, M., Allen, S.K., Boschung, J., Nauels, A., Xia, Y., Bex, V., Midgley, P.M. (Eds.), Climate Change 2013: the Physical Science Basis. Contribution of Working Group I to the Fifth Assessment Report of the Intergovernmental Panel on Climate Change. Cambridge University Press, Cambridge, United Kindom and New York, NY, USA, pp. 571–657.

Brandt, A.R., 2020. Accuracy of satellite-derived estimates of flaring volume for offshore oil and gas operations in nine countries. Environ. Res. Commun. 2, 051006.

Casadio, S., Arino, O., Serpe, D., 2012. Gas flaring monitoring from space using the ATSR instrument series. Rem. Sens. Environ. 116, 239–249.

Caseiro, A., Rucker, G., Tiemann, J., Leimbach, D., Lorenz, E., Frauenberger, O., Kaiser, J.W., 2018. Persistent hot spot detection and characterisation using SLSTR. Rem. Sens. 10 (7), 1118. https://doi.org/10.3390/rs10071118.

Caseiro, A., Gehrke, B., Rücker, G., Leimbach, D., Kaiser, J.W., 2020. Gas flaring activity and black carbon emissions in 2017 derived from the sentinel-3A Sea and land surface temperature radiometer. Earth Syst. Sci. Data 12, 2137–2155.

Chernov, A.A., 2016. Associated Gas Utilization Methods at Yurubcheno - Tokhomskoye Field. Bachelor thesis [In Russian]. Siberian Federal University, Institute of Oil and Gas, Departement of development and operation of oil and gas fields Krasnoyarsk. available online. http://elib.sfu-kras.ru/bitstream/handle/2311/29886/chernov_0_0.pdf?sequence. (Accessed 21 April 2020).

Cho, M.-H., Park, R.J., Yoon, J., Choi, Y., Jeong, J.I., Labzovskii, L., Fu, J.S., Huang, K., Jeong, S.-J., Kim, B.-M., 2019. A missing component of Arctic warming: black carbon from gas flaring. Environ. Res. Lett. 14, 094011.
Conrad, B.M., Johnson, M.R., 2017. Field measurements of black carbon yields from gas flaring. Environ. Sci. Technol. 51, 1893–1900.
Conrad, B.M., Johnson, M.R., 2019. Mass absorption cross-section of flare-generated black carbon: variability, predictive model, and implications. Carbon 149, 760–771.
Elvidge, C.D., Zhizhin, M., Baugh, K., Hsu, F.C., Ghosh, T., 2016. Methods for global survey of natural gas flaring from visible infrared imaging radiometer suite data. Energies 9 (1), 14. https://doi.org/10.3390/en9010014.
Elvidge, C.D., Bazilian, M.D., Zhizhin, M., Ghosh, T., Baugh, K., Hsu, F.C., 2018. The potential role of natural gas flaring in meeting greenhouse gas mitigation targets. Energy Strat. Rev. 20, 156–162.
Energas, 2016. Associated Gas of the Last Separation Stages. Compression of low-pressure APG, Neftegaz available online. http://en.energas.ru/pressroom/articles/poputnyy-gaz-poslednikh-stupeney-separatsii-komprimirovanie-nizkonapornogo-png/. (Accessed 24 January 2020).
Energas, 2018. Associated Petroleum Gas in Russia: the Road Will Be Mastered by the Going. Industrial and heating boiler rooms and mini-CHPP available online. http://en.energas.ru/pressroom/articles/poputnyy-neftyanoy-gaz-v-rossii-dorogu-osilit-idushchiy/. (Accessed 24 January 2020).
Evans, M., Roshchanka, V., 2014. Russian policy on methane emissions in the oil and gas sector: a case study in opportunities and challenges in reducing short-lived forcers. Atmos. Environ. 92, 199–206.
Evans, M., Kholod, N., Kuklinski, T., Denysenko, A., Smith, S.J., Staniszewski, A., Hao, W.M., Liu, L., Bond, T.C., 2017. Black carbon emissions in Russia: a critical review. Atmos. Environ. 163, 9–21.
Faruolo, M., Lacava, T., Pergola, N., Tramutoli, V., 2018. On the potential of the RST-FLARE algorithm for gas flaring characterization from space. Sensors 18 (8), 2466. https://doi.org/10.3390/s18082466.
Filippov, A., 2013. Cycle of articles "APG in Russia: Problems and solutions". Article No.3 "Chemical composition of associated gas", Neftegaz available online: http://en.energas.ru/pressroom/articles/komponentnyy-sostav-poputnogo-neftyanogo-gaza/. accessed on 06.03.2020.
Fisher, D., Wooster, M.J., 2018. Shortwave IR adaption of the mid-infrared radiance method of fire radiative power (FRP) retrieval for assessing industrial gas flaring output. Rem. Sens. 10, 305.
Government of Russian Federation, 2009. Government Decree No.7 Dated 8 January 2009, on Measures for Stimulating Reduction of Atmospheric Pollution with Products of Combustion of Associated Petroleum Gas in Flares [In Russian]. Government of Russian Federation, Moscow.
Government of Russian Federation, 2012. Government Decree No. 1148 Dated 8 November 2012, on Details for Accounting Payment for Emissions Formed during Flaring and (Or) Dispersing Associated Petroleum Gas [In Russian]. Government of Russian Federation, Moscow available online. https://cis-legislation.com/document.fwx?rgn=55810. accessed 12.04.2021.
Gvakharia, A., Kort, E.A., Brandt, A., Peischl, J., Ryerson, T.B., Schwarz, J.P., Smith, M. L., Sweeney, C., 2017. Methane, black carbon, and ethane emissions from natural gas flares in the bakken shale, north Dakota. Environ. Sci. Technol. 51, 5317–5325.
Hadley, O.L., Kirchstetter, T.W., 2012. Black-carbon reduction of snow albedo. Nat. Clim. Change 2, 437.
Harvard University. Oil & gas map. Available online: https://worldmap.harvard.edu/maps/6718. accessed on 03.10.2019.
Höglund-Isaksson, L., Gómez-Sanabria, A., Klimont, Z., Rafaj, P., Schöpp, W., 2020. Technical potentials and costs for reducing global anthropogenic methane emissions in the 2050 timeframe –results from the GAINS model. Environ. Res. Commun. 2, 025004.
Huang, K., Fu, J.S., Prikhodko, V.Y., Storey, J.M., Romanov, A., Hodson, E.L., Cresko, J., Morozova, I., Ignatieva, Y., Cabaniss, J., 2015. Russian anthropogenic black carbon: emission reconstruction and Arctic black carbon simulation. J. Geophys. Res.: Atmospheres 120 (11), 306–311, 333.
IEA, 2012. Energy Technology Perspectives 2012. IEA, Paris available online. https://www.iea.org/reports/energy-technology-perspectives-2012. (Accessed 9 September 2020).
IEA, 2019. Tracking Fuel Supply 2019. IEA, Paris available online. https://www.iea.org/reports/tracking-fuel-supply-2019. (Accessed 10 June 2020).
IIASA, 2020. Global emission fields of air pollutants and GHGs, ECLIPSE V6b available online. https://iiasa.ac.at/web/home/research/researchPrograms/air/Global_emissions.html. accessed on 12.04.2021.
Johnson, M.R., Devillers, R.W., Thomson, K.A., 2013. A generalized sky-LOSA method to quantify soot/black carbon emission rates in atmospheric plumes of gas flares. Aerosol. Sci. Technol. 47, 1017–1029.
Klimont, Z., Kupiainen, K., Heyes, C., Purohit, P., Cofala, J., Rafaj, P., Borken-Kleefeld, J., Schöpp, W., 2017. Global anthropogenic emissions of particulate matter including black carbon. Atmos. Chem. Phys. 17, 8681–8723.
Kühn, T., Kupiainen, K., Miinalainen, T., Kokkola, H., Paunu, V.V., Laakso, A., Tonttila, J., Van Dingenen, R., Kulovesi, K., Karvosenoja, N., Lehtinen, K.E.J., 2020. Effects of black carbon mitigation on Arctic climate. Atmos. Chem. Phys. 20, 5527–5546.
McEwen, J.D.N., Johnson, M.R., 2012. Black carbon particulate matter emission factors for buoyancy-driven associated gas flares. J. Air Waste Manag. Assoc. 62, 307–321.
Online GeoMaps of the Russian Federation (Open version), 2002. Map of mineral deposits (legend by Center "Mineral"). Research and Analytical Center "Mineral". Prepared according to the system of "Balance License" (FGBU "Rosgeolfond"), as well as public sources, scaleless, updated annually. Available online: https://openmap.mineral.ru/ (registration required), accessed on 03.10.2019.
PFC Energy, 2007. Using Russia's associated gas, prepared for the Global Gas Flaring Reduction Partnership and the World Bank available online: http://siteresources.worldbank.org/INTGGFR/Resources/pfc_energy_report.pdf. accessed on 21.04.2020.
Popovicheva, O.B., Evangeliou, N., Eleftheriadis, K., Kalogridis, A.C., Sitnikov, N., Eckhardt, S., Stohl, A., 2017. Black carbon sources constrained by observations in the Russian high arctic. Environ. Sci. Technol. 51, 3871–3879.
Rosgeolfond (Russian Federal Geological Fund). Rosgeolfond database [In Russian]. Available online. https://www.rfgf.ru/bal/a/. accessed on 3.10.2019.
Rosneft, Annual reports Available online: https://www.rosneft.com/Investors/Reports_and_presentations/Annual_reports/, accessed on 03.10.2019.
Rosreestr (Federal Service for State Registration Cadastre and Cartography of Russia), 2011. Public Cadastrial Map [In Russian]. Available online: https://pkk5.rosreestr.ru. accessed on 03.10.2019.
Sand, M., Berntsen, T.K., von Salzen, K., Flanner, M.G., Langner, J., Victor, D.G., 2016. Response of Arctic temperature to changes in emissions of short-lived climate forcers. Nat. Clim. Change 6, 286–289.
Saunier, S., Bergauer, M.-A., Isakova, I., 2019. Best Available Techniques Economically Achievable to Address Black Carbon from Gas Flaring: EU-Funded Action on Black Carbon in the Arctic – Technical Report 3. October 2019, p. 44. available online. https://www.amap.no/documents/doc/best-available-techniques-economically-achievable-to-address-black-carbon-from-gas-flaring-available-in-english-russian/2058. (Accessed 22 December 2020).
Sharma, A., Wang, J., Lennartson, E.M., 2017. Intercomparison of MODIS and VIIRS fire products in khanty-mansiysk Russia: implications for characterizing gas flaring from space. Atmosphere 8 (6), 95. https://doi.org/10.3390/atmos8060095.
Shindell, D., Kuylenstierna, J.C.I., Vignati, E., van Dingenen, R., Amann, M., Klimont, Z., Anenberg, S.C., Muller, N., Janssens-Maenhout, G., Raes, F., Schwartz, J., Faluvegi, G., Pozzoli, L., Kupiainen, K., Höglund-Isaksson, L., Emberson, L., Streets, D., Ramanathan, V., Hicks, K., Oanh, N.T.K., Milly, G., Williams, M., Demkine, V., Fowler, D., 2012. Simultaneously mitigating near-term climate change and improving human health and food security. Science 335, 183–189.
Stohl, A., Klimont, Z., Eckhardt, S., Kupiainen, K., Shevchenko, V.P., Kopeikin, V.M., Novigatsky, A.N., 2013. Black carbon in the Arctic: the underestimated role of gas flaring and residential combustion emissions. Atmos. Chem. Phys. 13, 8833–8855.
Stohl, A., Aamaas, B., Amann, M., Baker, L.H., Bellouin, N., Berntsen, T.K., Boucher, O., Cherian, R., Collins, W., Daskalakis, N., Dusinska, M., Eckhardt, S., Fuglestvedt, J.S., Harju, M., Heyes, C., Hodnebrog, O., Hao, J., Im, U., Kanakidou, M., Klimont, Z., Kupiainen, K., Law, K.S., Lund, M.T., Maas, R., MacIntosh, C.R., Myhre, G., Myriokefalitakis, S., Olivie, D., Quaas, J., Quennehen, B., Raut, J.C., Rumbold, S.T., Samset, B.H., Schulz, M., Seland, O., Shine, K.P., Skeie, R.B., Wang, S., Yttri, K.E., Zhu, T., 2015. Evaluating the climate and air quality impacts of short-lived pollutants. Atmos. Chem. Phys. 15, 10529–10566.
The World Bank, 2019. Global gas flaring inches higher for the first time in five years. Available online: https://blogs.worldbank.org/opendata/global-gas-flaring-inches-higher-first-time-five-years. accessed on 10.06.2020.
The World Bank, 2020. Global Gas Flaring Reduction Partnership (GGFR). Available online: https://www.worldbank.org/en/programs/gasflaringreduction. accessed on 10.06.2020.
U.S. Energy Information Administration, 2017. Country Analysis Brief: Russia. U.S. Energy Information Administration available online. https://www.eia.gov/international/analysis/country/RUS. (Accessed 18 February 2020).
U.S. Energy Information Administration (EIA), 2020. Russia, Petroleum and Other Liquids, Data on Annual Production. U.S. Energy Information Administration (EIA) available online. https://www.eia.gov/international/data/country/RUS/petroleum-and-other-liquids/annual-petroleum-and-other-liquids-production?pd=5&p=0000000000000000000000000000000vg&u=0&f=A&v=mapbubble&a=-&i=none&vo=value&t=C&g=none&l=249–197&s=94694400000&e=1577836800000&. (Accessed 17 December 2020).
Wang, J., Roudini, S., Hyer, E.J., Xu, X., Zhou, M., Garcia, L.C., Reid, J.S., Peterson, D.A., da Silva, A.M., 2020. Detecting nighttime fire combustion phase by hybrid application of visible and infrared radiation from Suomi NPP VIIRS. Rem. Sens. Environ. 237, 111466.
Wikimapia, available online: http://wikimapia.org/#lang=en, accessed on 03.10.2019.
Zhang, X., Scheving, B., Shoghli, B., Zygarlicke, C., Wocken, C., 2015. Quantifying gas flaring CH4 consumption using VIIRS. Rem. Sens. 7, 9529–9541.
Zhizhin, M., Elvidge, C.D., Davis, M., 2019. Reading Gas Flare Histories with VIIRS Nightfire Temporal Profiles: Preliminary Results. AGU Fall meeting, San Francisco, CA, USA, pp. B13F–B2432 available online. https://agu.confex.com/agu/fm19/meetingapp.cgi/Paper/554512. (Accessed 29 June 2020).